

Adsorption of silicon atom on chlorinated Si(100) surface

E. S. Skorokhodov^{1,2}, T. V. Pavlova^{1,*}, G. M. Zhidomirov^{1,3}, and K. N. Eltsov¹

¹*Prokhorov General Physics Institute of the Russian Academy of Sciences, Moscow, Russia*

²*Moscow Institute of Physics and Technology, Dolgoprudny, Russia and*

³*Faculty of Physics, National Research University Higher School of Economics, Moscow, Russia*

Homoepitaxial growth of Si on Si(100) covered by a resist mask is a necessary technological step for the fabrication of donor-based quantum devices with STM lithography. Using density functional theory, we investigated the adsorption of a single silicon atom on Si(100)-2×1-Cl as the starting process of Si epitaxy. The incorporation of a silicon atom under Cl monolayer proved to be the most energetically favorable process. In the course of spontaneous adsorption, one Si adatom substitutes one Cl atom. Then, the adatom can migrate to more stable adsorption sites forming bonds with two Si and two Cl atoms, but this process requires activation energy. In addition, we found that at Si adsorption, SiCl₂, SiCl₃, and SiCl₄ clusters can be formed above a Si(100)-2×1-Cl surface. SiCl₂ clusters are bound weakly to the substrate, and their desorption leaves the silicon surface free of chlorine. Our results show that chlorine segregates to the surface during Si deposition and does not incorporate into homoepitaxial layers.

PACS numbers: 68.43.Bc, 68.43.Fg

I. INTRODUCTION

Homoepitaxy of silicon is widely utilized for dopant encapsulation in atomic scale devices. Sufficiently thick crystalline silicon layer (about 50 nm) should be grown on top of a surface with dopants to preserve the electronic properties of semiconducting devices from unwanted surface effects. Silicon epitaxy is a necessary step for the fabrication of δ -layers^{1,2}, nanowires^{3,4}, and quantum dots⁵. In addition, a high quality of epitaxial layers is extremely important for phosphorus-in-silicon quantum computer building blocks^{6,7}.

To create the desired two-dimensional structure of impurities, a silicon surface is covered with a resist and then the resist is patterned with a scanning tunneling microscope (STM) tip. After the adsorption of molecules containing specific impurities, the impurity atoms are embedded on the resist-free sites and then the surface is covered with epitaxial silicon layers. The quality of epitaxial layers strongly depends on the interaction of Si adatoms with atoms of the resist used for mask fabrication. If a hydrogen monolayer is used as a mask for the patterning of Si(100)-2×1 surface, the uniform growth of an epitaxial Si film is suppressed at room temperature^{8,9} due to low mobility of Si adatoms¹⁰. The surface roughness of the film can be decreased by sample heating, as in the case of Si epitaxy on clean Si(100)¹¹. However, to prevent the lateral diffusion of dopants, heating to temperatures at which hydrogen begins to desorb (above 400°C¹²) should be avoided.

Theoretical calculations of Si atoms adsorption and diffusion on H-terminated Si(100)-2×1 surface have provided insight into mechanism of homoepitaxy^{10,13,14}. A silicon atom adsorbed on Si(100)-2×1-H can spontaneously substitute a hydrogen atom on the surface and then form Si dihydride. Experimental results confirm the presence of surface Si dihydrides at sub-monolayer coverages¹⁵. As such a Si film grows, most H atoms seg-

regate to the surface and are not incorporated into the epitaxial film^{11,16}.

Chlorine monolayer on a silicon surface can also be utilized as a resist^{17,18}. Of particular interest is a proposal to use STM lithography on Si(100)-2×1-Cl for placing P atoms with atomic precision¹⁹. However, the atomic processes of silicon epitaxy on a Cl-terminated Si(100)-2×1 surface have not been studied either theoretically or experimentally.

In this paper, we report the results of density functional theory (DFT) calculations of Si atom adsorption on Si(100)-2×1-Cl. A silicon adatom spontaneously substitutes a Cl atom and further migrates to the most stable inter-bridge dimer site (bound with two Si and two Cl atoms). This process is similar to that in the case of Si(100)-2×1-H surface, and should lead to Cl atoms segregation during Si epitaxy. Despite the small radius of hydrogen being suggested¹³ as a reason for spontaneous substitutional adsorption of silicon on Si(100)-2×1-H, the same adsorption mechanism is found to work for a chlorinated silicon surface. Moreover, there is an additional pathway of spontaneous Si adsorption with formation of SiCl₂ clusters weakly bound with the silicon surface. The spontaneous desorption of SiCl₂ clusters from the surface makes it possible to remove chlorine without annealing.

II. CALCULATION METHOD

First-principle calculations of silicon atom adsorption on Si(100)-2×1-Cl surface were performed with spin-polarized density functional theory implemented in VASP^{20,21}. The generalized gradient approximation with the exchange-correlation functional in the form of Perdew–Burke–Ernzerhof (PBE) was applied²². The eigenfunctions of valence electrons were expanded in a plane waves basis set with an energy cutoff of 350 eV. The Si(100) surface was simulated by recurring 4×4 cells

consisted of eight atomic layers of silicon. The slabs were separated by vacuum gaps of approximately 15 Å. The bottom three layers were fixed at bulk positions, while the other silicon layers were allowed to relax. The lowest layer was covered by hydrogen atoms to saturate the broken bonds of silicon. Chlorine atoms were placed on the upper side of the slab to form a Si(100)-2×1-Cl structure. Reciprocal cell integrations were performed using the 4×4×1 k-points grid.

The adsorption energy (E_{ads}) of a silicon adatom was calculated as the difference between the total energy of the slab with the adatom ($E_{Si+surf}$) and the total energies of the Si(100)-2×1-Cl surface (E_{surf}) and a Si atom in the gaseous phase (E_{Si}):

$$E_{ads} = E_{Si+surf} - E_{surf} - E_{Si}. \quad (1)$$

The activation barriers (E_{act}) were calculated using the NEB (nudged elastic band) method²³ implemented in VASP.

III. RESULTS

To investigate a potential energy surface for Si adsorption on Si(100)-2×1-Cl, Si adatom (Si_{ad}) was placed 2.50 Å above the chlorine monolayer (Fig. 1a). Eight different initial configurations (A_0 – H_0) of the silicon adatom above the Si(100)-2×1-Cl surface were tested (Fig. 1b). Structures A–H obtained after the optimization of the corresponding initial configurations A_0 – H_0 are shown in Fig. 2.

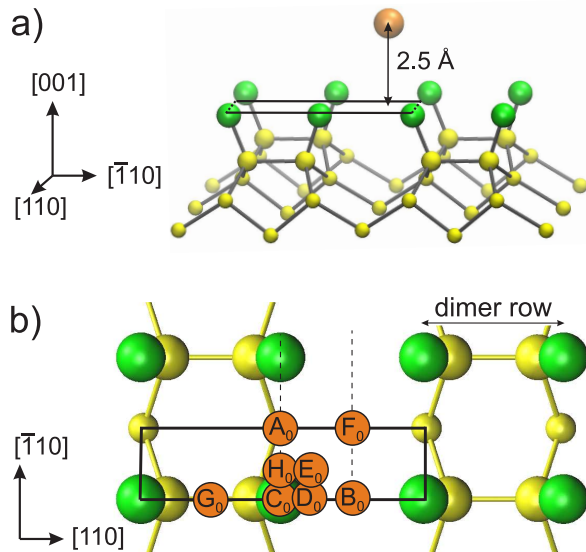


Figure 1. Perspective (a) and top (b) views of initial configurations of Si(100)-2×1-Cl with Si adatom above the surface. Silicon bulk and surface atoms are small and big yellow circles, respectively; chlorine atoms are green circles; Si adatom is orange circle.

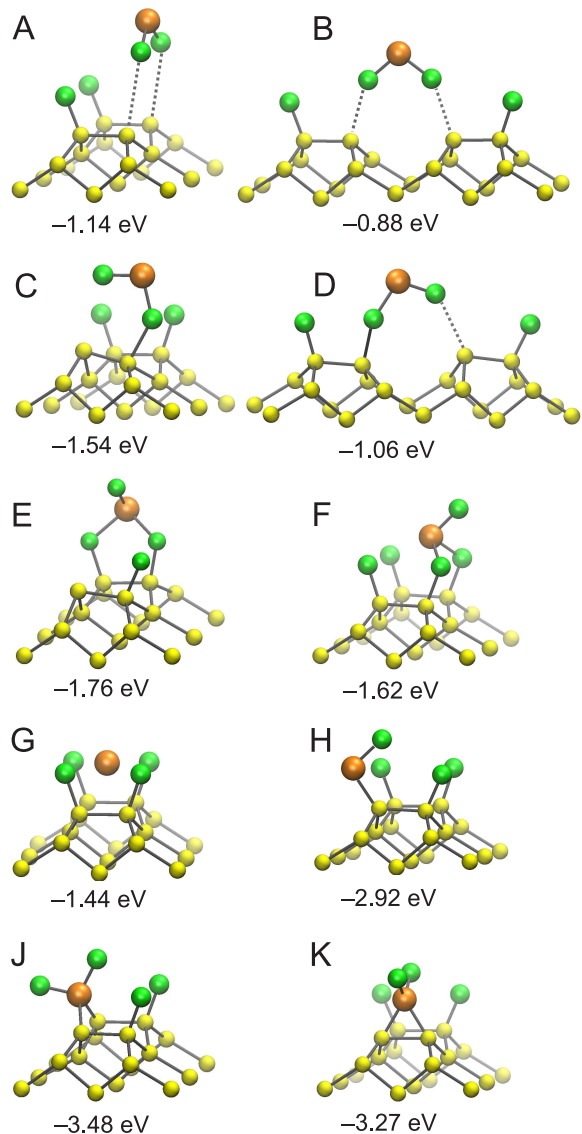


Figure 2. Optimized atomic structures and their adsorption energies for Si adsorbed on Si(100)-2×1-Cl. Structures A–H were obtained as a result of the relaxation of the coordinates when the Si adatom was in the initial positions A_0 – H_0 (Fig. 1b), whereas for structures J and K adatom was initially placed close to the final positions.

In symmetric positions A_0 and B_0 (Fig. 1b), the adatom forms two equivalent bonds with Cl atoms belonging to different dimers (structures A and B in Fig. 2). Both optimized models (A and B) have the same Si–Cl bond lengths (2.09 Å) and the Cl– Si_{ad} –Cl angle of 102°. These structural parameters appear to be equal to those calculated for the $SiCl_2$ molecule in vacuum (2.09 Å and 102°). Note also that the formation of the $SiCl_2$ clusters is accompanied by the lengthening of the distances between Cl and Si surface atoms. In particular, the Cl–Si distances for models A and B are 4.28 Å and 3.26 Å, respectively, which is longer than the Si–Cl bond length

of an unperturbed Si(100)-2×1-Cl surface (2.08 Å). This effect indicates a rather weak interaction of the SiCl₂ cluster with the surface. However, the adsorption energies of the Si adatom remain negative for models A and B (−1.14 eV and −0.88 eV, respectively).

Two other SiCl₂ clusters were obtained from the Si_{ad} initial adsorption position on top of a Cl atom (C₀ in Fig. 1b) and from a position shifted by 0.50 Å across the dimer row (D₀ in Fig. 1b). However, the geometry of SiCl₂ clusters in models C and D (Fig. 2) differs from that of a SiCl₂ molecule. Indeed, in model C (model D), the distance between the Si_{ad} and the upper chlorine atom is 2.06 Å (2.03 Å), whereas the distance between the Si_{ad} and the lower chlorine atom appears to be higher — 2.18 Å (2.25 Å). The angle Cl–Si_{ad}–Cl (104°) is close to that in the SiCl₂ molecule (102°). Models C and D have one of the bonds between the SiCl₂ cluster and the substrate silicon atom shorter than those in models A and B, respectively: the corresponding Cl–Si distances for models C and D are 2.57 Å and 2.41 Å, being much shorter than in models A (4.28 Å) and B (3.26 Å). Additionally, in model C (model D), the bond length between the upper chlorine atom of the SiCl₂ cluster and the silicon atom of the surface is increased to 3.89 Å (3.54 Å) compared with the Si–Cl bond length (2.08 Å) before the Si adsorption.

The other stable cluster, SiCl₃, was obtained by optimizing initial configurations E₀ and F₀ in Fig. 1b. In model F (Fig. 2), the SiCl₃ cluster forms as a Cl atom is taken from the nearest dimer (not shown in Fig. 2) and added to the cluster. The shortest bond in such a SiCl₃ cluster is between the Si_{ad} and the upper Cl (2.08 Å), whereas the lengths of the other two Si_{ad}–Cl bonds are 2.49 Å. The distance between the lower Cl atoms of the SiCl₃ cluster and Si surface atoms is 2.21 Å. Note that the SiCl₃ cluster located on a bridge dimer site (model E in Fig. 2) is energetically more favorable (−1.76 eV) than that in the inter-bridge dimer site (−1.62 eV, model F in Fig. 2).

The optimization of the initial configuration G₀ in Fig. 1b leads to the formation of the SiCl₄ cluster (see model G in Fig. 2). In this case, all Si_{ad}–Cl bonds are equivalent and characterized by the length of 2.70 Å. Adsorption energy in the model G (−1.44 eV) appears to be compatible with E_{ads} calculated for configurations containing SiCl₂ and SiCl₃ clusters (see Fig. 2).

Optimizing initial configuration H₀ (Fig. 1b), we get a Si adatom embedding in the silicon lattice, and the chlorine segregated on top of the surface structure (model H in Fig. 2). The bond length between the Si adatom and the nearest Si atom is a little longer than in the bulk (2.50 Å vs 2.37 Å). The bond between the adatom and the second-layer substrate atom is also longer, 3.80 Å. The Si_{ad}–Cl bond length (2.09 Å) appears to be close to the reference Si–Cl values of the bond length of an unperturbed Si(100)-2×1-Cl surface. Therefore, of all structures formed during spontaneous adsorption of a silicon atom from positions indicated in Fig. 1b, substitu-

tional adsorption leads to the most energetically favorable structure H ($E_{ads} = -2.92$ eV).

Since such substitutional adsorption turned out to be very stable, we have considered additional adsorption positions of a silicon atom under the chlorine monolayer, that could be reached by Si_{ad} migration from position H. In the most favorable configurations, Si_{ad} forms SiCl₂ clusters in the inter-bridge and bridge dimer sites (models J and K in Fig. 2). In these models, the Si_{ad} bonds with Si surface atoms, unlike models A–G, in which it bonds with Cl atoms only. The Si_{ad}–Si bond lengths are 2.44 Å and 2.36 Å in inter-bridge and bridge sites, respectively, while the Si_{ad}–Cl bond lengths are 2.05 Å for both sites. The adsorption energies calculated for models J and K are −3.48 eV and −3.27 eV, respectively. This result strongly suggests that the formation of the Si_{ad}–Si bonds makes a valuable contribution to the lowering of the adsorption energy in comparison with the formation of Si_{ad}–Cl bonds only. Thus, atomic configuration J appears to be the most stable structure of all considered in this paper.

Figure 3 shows the energy diagram describing the processes of Si_{ad} adsorption on Si(100)-2×1-Cl and desorption of SiCl₂, SiCl₃, and SiCl₄ clusters. The lower part of the diagram corresponds to the formation of bonds between the Si adatom and Si and Cl atoms (Cl–Si_{ad}–Si), while the upper part shows the formation of bonds between the adatom and Cl atoms only (Si_{ad}–Cl).

All the structures in the upper part of the diagram (Fig. 3) can be formed as a result of spontaneous adsorption. For each cluster, we have tested possible desorption paths. In models A and C, a SiCl₂ cluster desorbs over a rather low activation barrier ($E_{act} \lesssim 0.1$ eV), while in models B and D, it desorbs spontaneously, without any barrier. Therefore, as soon as a SiCl₂ cluster forms on the surface, it can desorb as a SiCl₂ molecule.

The SiCl₃ cluster desorbs from configuration F over the activation barrier equal to the energy difference between the initial and final states. However, this difference is bigger (1.57 eV) than that of the SiCl₂ desorption. A SiCl₄ cluster can desorb from model G, but it requires the highest activation barrier of 3.09 eV.

Formation of bonds between the adatom and Si surface atoms stabilizes the structure, putting models H, J, and K in the lower part of the diagram (Fig. 3). Configuration H may be the result of the spontaneous relaxation of initial model H₀ (Fig. 1), but also of a transition from configuration B without any activation barrier. Further, the Si adatom adsorbed in the substitutional site can attach a chlorine atom from the nearest dimer and migrate to the most stable inter-bridge dimer site (model J). However, this pathway requires the activation energy of 0.71 eV. The alternative process is the adatom transition to the SiCl₂ cluster in the bridge dimer site (model K). This process would not be the energetically preferred one, since model K is less favorable by 0.21 eV and the activation barrier for an H→K transition is higher by 0.08 eV than that for an H→J transition.

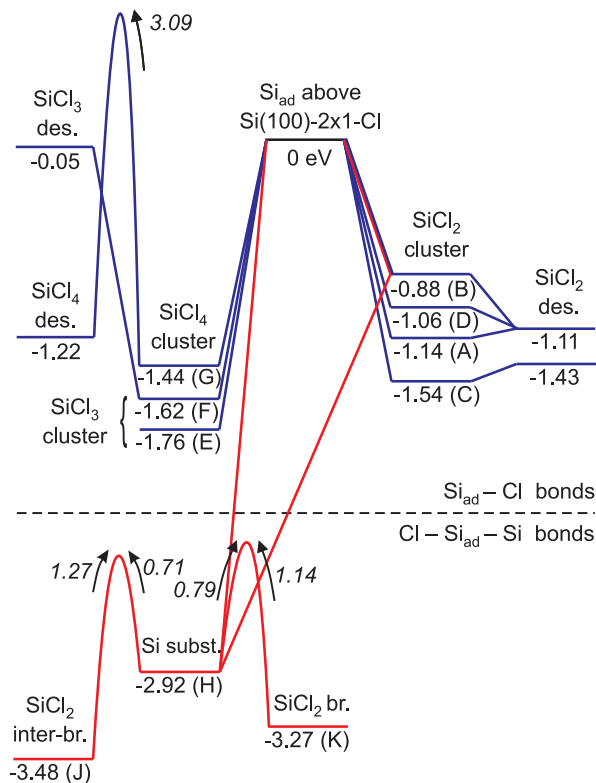


Figure 3. Potential energy diagram for Si adsorption on Si(100)-2 \times 1-Cl and SiCl₂, SiCl₃, and SiCl₄ desorption. Reaction pathways with Cl-Si_{ad}-Si bond formation are shown by red lines, adsorption and desorption pathways with Si_{ad}-Cl bonds by blue lines. Activation barriers are indicated by arrows (energy barriers less than 0.05 eV are not shown in the diagram).

The SiCl₂ molecular desorption from the most stable configurations J and K requires the activation energy not less than the energy difference between the initial (-3.48 eV and -3.27 eV, respectively) and final states (-1.11 eV and -1.14 eV, respectively). This difference is about 2 eV, which means that SiCl₂ desorption from structures J and K is highly suppressed compared with SiCl₂ desorption from structures A-D.

IV. DISCUSSION

In this section, we turn to the comparison of Si adsorption on a Cl-terminated Si(100)-2 \times 1 surface with a H-terminated one. In the latter case, the Si adatom, spontaneously substituting a hydrogen atom¹³, can capture one more H atom and form a SiH₂ cluster in a bridge dimer or an inter-bridge dimer site. The adsorption energies of these structures are lower than that of the substitutional adsorption structure by 0.5 eV and 0.6 eV, respectively, and the activation barriers for Si adatom transition from the substitutional site to SiH₂ cluster in the

bridge dimer or inter-bridge dimer site are 0.5 eV and 0.6 eV, respectively¹⁵. At room temperature, most of the adsorbed Si atoms transfer from the substitutional site to the bridge dimer site due to the low activation energy (0.5 eV). Further diffusion of the SiH₂ cluster into the most favorable position in the inter-bridge dimer site requires an activation energy of 1.1 eV, which can be hardly overcome at room temperature. This scenario is in agreement with the experiment¹⁵, where Si atoms deposited on a H-terminated Si(100)-2 \times 1 surface at room temperature were found predominantly in the bridge dimer sites.

Like in the previous case, a silicon atom adsorbed on a Si(100)-2 \times 1-Cl surface spontaneously substitutes a chlorine atom (model H in Fig. 2). Then the Si adatom can capture an additional chlorine atom, thus creating the more stable configurations with a SiCl₂ cluster (models J and K in Fig. 2). According to our calculations, the minimum energy path from model H to model K requires an activation energy of 0.79 eV, whereas the transition from model H to the most stable structure (model J) requires only 0.71 eV. Thus, our results indicate that most Si adatoms deposited on a Si(100)-2 \times 1-Cl surface at room temperature are adsorbed into the inter-bridge dimer site, while on a Si(100)-2 \times 1-H surface Si adatoms occupy mostly the bridge dimer sites.

Another difference between Si adsorption on Si(100)-2 \times 1-Cl and Si(100)-2 \times 1-H is that in the formed case, SiCl₂ clusters weakly bound to the Cl-terminated surface are formed. A SiCl₂ molecule can easily desorb from structures A-D containing SiCl₂ clusters, since the energy barriers appear to be very low (\lesssim 0.1 eV) or even non-existent. The desorption of the SiCl₂ species leads to the partial removal of chlorine from a Si(100)-2 \times 1-Cl surface, and the subsequent Si overgrowth on the substrate area free of Cl should increase the adatom mobility (for example, the Si adatom mobility on Si(100)-2 \times 1 surfaces terminated by hydrogen¹⁰ and bromine²⁴ is lower than that on a clean surface). This in turn leads to a more uniform growth of the epitaxial layer. The low temperature removal of Cl will not lead to the diffusion of dopants (for example, P atoms) on the surface.

Therefore, when compared to the common practice of using a hydrogen monolayer as a resist, a chlorine monolayer presents not just analogies, but also potential advantages because of low temperature removal of chlorine during Si epitaxy. Firstly, spontaneous substitutional adsorption takes place both on H-¹⁵ and Cl-terminated Si(100)-2 \times 1. Secondly, the most stable sites for Si_{ad} on H-¹⁵ (or Cl-) terminated surfaces are bridge and inter-bridge dimer sites, where the Si_{ad} is bound to two Si and two H (or Cl) atoms. Thirdly, the energy barriers for Si transition from the substitutional adsorption site to these stable sites are similar for hydrogen (0.5-0.6 eV¹⁵) and chlorine (0.7-0.8 eV) monolayers. Fourthly, we have found out that SiCl₂ clusters formed during silicon adsorption can easily desorb from a Cl-terminated surface. Thus, depositing silicon on a chlorine monolayer should produce silicon epitaxial layers of quality at least not

worse (may be even better) than on a hydrogen monolayer.

V. CONCLUSIONS

The structures and energetics of Si adsorption on Si(100)-2×1-Cl have been studied with the density function theory. The activation barriers for transitions between the most stable states and desorption of different SiCl_x compounds from the surface have been calculated. A Si adatom adsorbed on a Si(100)-2×1-Cl surface spontaneously substitutes a Cl atom (more preferable) or forms SiCl₂, SiCl₃, and SiCl₄ clusters. Note that the SiCl₂ clusters are bound weakly to the surface and therefore can easily desorb. A Si adatom located in the substi-

tutional site can migrate to the most stable inter-bridge dimer site with the activation energy of 0.71 eV.

Thus, our results indicate that chlorine segregates to the surface during Si deposition and is not incorporated into the epitaxial layers. Moreover, Si deposition on a Cl-terminated surface has a potential advantage compared to a H-terminated surface, since it may improve the quality of low temperature silicon epitaxy.

VI. ACKNOWLEDGEMENT

The work was supported by Russian Science Foundation (grant 16-12-00050). We also thank the Joint Supercomputer Center of RAS for providing the computing power.

-
- * pavlova@kapella.gpi.ru
- ¹ T.-C. Shen, J.-Y. Ji, M. A. Zudov, R.-R. Du, J. S. Kline, and J. R. Tucker, *Appl. Phys. Lett.* **80**, 1580 (2002).
 - ² J. Keizer, S. Koelling, P. Koenraad, and M. Simmons, *ACS Nano* **9**, 2537 (2015).
 - ³ B. Weber, S. Mahapatra, H. Ryu, S. Lee, A. Fuhrer, T. Reusch, D. L. Thompson, W. C. T. Lee, G. Klimeck, L. C. L. Hollenberg, and M. Simmons, *Science* **335**, 64 (2012).
 - ⁴ B. Weber, H. Ryu, Y.-H. M. Tan, G. Klimeck, and M. Y. Simmons, *Phys. Rev. Lett.* **113**, 246802 (2014).
 - ⁵ M. Fuechsle, J. Miwa, S. Mahapatra, H. Ryu, S. Lee, O. Warschkow, L. C. L. Hollenberg, G. Klimeck, and M. Simmons, *Nat. Nanotechnol.* **7**, 242 (2012).
 - ⁶ L. Oberbeck, N. J. Curson, M. Y. Simmons, R. Brenner, A. R. Hamilton, S. R. Schofield, and R. G. Clark, *Appl. Phys. Lett.* **81**, 3197 (2002).
 - ⁷ M. A. Broome, S. Gorman, M. House, S. Hile, J. Keizer, D. Keith, C. D. Hill, T. Watson, W. Baker, L. C. L. Hollenberg, and M. Simmons, *Nature Communications* **9** (2018).
 - ⁸ D. P. Adams, S. M. Yalisove, and D. J. Eaglesham, *Appl. Phys. Lett.* **63**, 3571 (1993).
 - ⁹ L. Oberbeck, T. Hallam, N. J. Curson, M. Y. Simmons, and R. G. Clark, *Appl. Surf. Sci.* **212–213**, 319 (2003).
 - ¹⁰ J. Nara, T. Sasaki, and T. Ohno, *Phys. Rev. Lett.* **79**, 4421 (1997).
 - ¹¹ X. Deng, P. Namboodiri, K. Li, X. Wang, G. Stan, A. F. Myers, X. Cheng, T. Li, and R. M. Silver, *Appl. Surf. Sci.* **378**, 301 (2016).
 - ¹² M. L. Yu, D. J. Vitkavage, and B. S. Meyerson, *J. Appl. Phys.* **59**, 4032 (1986).
 - ¹³ S. Jeong and A. Oshiyama, *Phys. Rev. Lett.* **79**, 4425 (1997).
 - ¹⁴ S. Jeong and A. Oshiyama, *Phys. Rev. B* **58**, 12958 (1998).
 - ¹⁵ H. Kajiyama, Y. Suwa, S. Heike, M. Fujimori, J. Nara, T. Ohno, S. Matsuura, T. Hitosugi, and T. Hashizume, *J. Phys. Soc. Jpn.* **74**, 389 (2005).
 - ¹⁶ J.-Y. Ji and T.-C. Shen, *Phys. Rev. B* **70**, 115309 (2004).
 - ¹⁷ S. Moon, C. Jeon, H. Hwang, C. Hwang, H. Song, H. Shin, S. Chung, and C. Park, *Adv. Mater.* **19**, 1321 (2007).
 - ¹⁸ C. Jeon, H.-N. Hwang, H.-J. Shin, C.-Y. Park, and C.-C. Hwang, *Appl. Surf. Sci.* **257**, 8794 (2011).
 - ¹⁹ T. V. Pavlova, G. M. Zhidomirov, and K. N. Eltsov, *J. Phys. Chem. C* **122**, 1741 (2018).
 - ²⁰ G. Kresse and J. Hafner, *Phys. Rev. B* **47**, 558 (1993).
 - ²¹ G. Kresse and J. Furthmüller, *Phys. Rev. B* **54**, 11169 (1996).
 - ²² J. P. Perdew, K. Burke, and M. Ernzerhof, *Phys. Rev. Lett.* **77**, 3865 (1996).
 - ²³ H. Jónsson, G. Mills, and K. W. Jacobsen, “Nudged elastic band method for finding minimum energy paths of transitions,” in *Classical and Quantum Dynamics in Condensed Phase Simulations*, edited by B. J. Berne, G. Ciccotti, and D. F. Coker (1998) pp. 385–404.
 - ²⁴ G. J. Xu and J. H. Weaver, *Phys. Rev. B* **70**, 165321 (2004).